

Wildfire Research

Performance of Fire-Retardant Coatings Used in Exterior Applications

Stephen L. Quarles, Ph.D.
Christine D. Standohar-Alfano, Ph.D.

OCTOBER 2017

ACKNOWLEDGEMENTS

The combustibility tests reported here were conducted at the University of North Carolina at Charlotte. The contributions of Professor Aixi Zhou, Ph.D., and graduate students, Mr. Babak Bahrani and Mr. Vahid Hemmati, are gratefully acknowledged.

Introduction

The U.S. loses approximately 3,000 homes due to wildfires every year (Maranghides et al., 2015). As building development continues in wildland-prone areas, communities will continue to be at risk from wildfires. In addition, since 2000, the wildfire season has lengthened with bigger, more damaging events (Short, 2015; Gorte, 2013).

Buildings threatened by wildfire can be mitigated through the development of a strategy that address the built environment, vegetation, and other combustible materials on the property. Use of noncombustible materials and ember-resistant design features are examples of strategies that reduce the vulnerability of buildings to wildfire.

Mitigation strategies typically include active and passive measures. Active measures require an automatic or manual action to implement. Examples of active measures can include routine maintenance items, such as maintaining landscape vegetation to remove dead branches and removing accumulated pine needles from gutters. Some active measures are only undertaken when a wildfire threatens. These measures could include turning on an exterior sprinkler system, or covering up attic and crawl space vents. Passive measures differ in that they do not require any additional action by the resident or firefighting personnel (or other first responders) to activate when a wildfire threatens. Examples of passive measures include use of noncombustible materials for siding and a Class A fire-rated roof covering, installation of multi-paned windows with tempered glass, and installing vents that have demonstrated resistance to the intrusion of wind-blown embers.

In buildings where combustible siding has been installed, fire-retardant coatings could be used to reduce their vulnerability to wildfire exposures, particularly radiant heat and flame contact exposures. Commercially available coatings include fire-retardant gel products that can be applied by a resident or first responder. Since the length of time that a gel product is effective after application is on the order of hours, it would be considered an active mitigation measure and would be applied only when a wildfire threatens. Other fire-retardant coatings, both film-forming paints and penetrating types, have been reported to have an effective service life on the order of years. Since these are more permanent, they would fit more appropriately in the passive mitigation strategy category. If effective, these longer-term coatings (both film forming and penetrating types) would arguably be less expensive than, for example, removing combustible siding and replacing with a noncombustible type.

Many of the longer-term, fire-retardant, film-forming paints and penetrating coatings are intumescent types. When heat is applied to intumescent coatings, they swell up to 20 times their original dry-film coating thickness, creating an insulating layer that provides protection that is effective until the layer is consumed (Bahrani, 2015). There is limited information on the long-term performance of intumescent coatings intended for

use in an exterior application. White and Diertenberger (2010) reported that studies have shown that coatings have uncertain effective service lives when used in an exterior location and would therefore need to be reapplied regularly. Acknowledging the uncertain performance of coatings, the use of coatings is not allowed for compliance with provisions of Chapter 7A of the California Building Code (2009).

When used in exterior applications, the fire-retardant coating is subjected to changes in temperature, humidity, solar radiation, and other weathering factors. This weathering can negatively impact the fire-retardant performance due to surface erosion or other forms of coating degradation, potentially resulting in a reduction of the fire-retardant properties before the end of the anticipated effective service life. For this reason, an experiment was designed to evaluate changes in the fire performance of coatings applied to an otherwise untreated wood substrate as a function of outdoor weathering. The coating products selected for use in this experiment were reported in product literature to have an effective service life of up to five years when used in an exterior location.

Experimental Procedure

An internet search found that there were approximately 15 fire-retardant (largely intumescent) coatings marketed for use in light-frame wood construction. Of these, about half were marketed as appropriate for use in interior and exterior applications. Five coating products were selected for use in this experiment. The selected products, each with an expected service life of up to five years in an exterior location, represented a majority of the exterior-use coating products found.

Application of the coating and weathering was performed at the Insurance Institute for Business & Home Safety (IBHS) Research Center in Richburg, South Carolina. Tests to evaluate fire performance of the coatings were conducted using a cone calorimeter located at the University of North Carolina at Charlotte (UNC Charlotte). Comparisons were made for product performance over different durations of outdoor weathering time up to 12 months. The fire performance of weathered samples was compared to tests performed on uncoated, non-weathered samples. Time to ignition (TTI), time to intumescence (T_{intu}), and peak heat release rate (PHRR) were used to evaluate performance. Manufacturer-supplied performance information for all coating products used in these experiments were limited to a flame spread index obtained from tests conducted on a coated substrate following procedures outlined in ASTM E84. They all reported Class A performance. Flame spread was not evaluated in the experiments reported here.

Material and Coating Type

Five coating products were selected for use in this study. Based on product information provided by the manufacturer, all were expected to be effective for up to five years when used in an exterior environment. All products were fire-retardant; four of the products were reported to have intumescent characteristics. The products were designated using letters A through E. Three of the intumescent products were film-forming products (i.e., paints) and assigned letters A, B, and C. Products D and E were penetrants; rather than forming a film, these products penetrated the wood and left only a very thin layer on the surface. Product D was the product with non-intumescent characteristics.

The surfaces of all coated specimens were evaluated. Uncoated specimens were used as a control to establish the baseline and more accurately determine the performance of the products. Products A, B, and C—all film-forming coatings—were also the focus of testing for combustibility and coating thickness. Throughout the remainder of this report, the term *coatings* will be used generically to refer to either film-forming or penetrant (non-film-forming) products.

Using a paintbrush, the coatings were applied to 4-ply, AC-grade, southern yellow pine plywood panels that had a nominal thickness of 0.5 in. (12.5 mm). The fire-retardant coating products were each applied to three different 4-ft x 8-ft (1.2-m x 2.4-m) plywood panels. The non-weathered backside (C-grade side) and the four edges of each panel were painted with one layer of regular, semi-gloss white primer to provide some protection against the absorption of water and, therefore, minimize the associated dimensional change on the non-weathered side of the wood. This was important because test specimens were smaller than typical sizes of siding material. Smaller specimens will have more exposed edge relative the surface area of larger samples. The fire-retardant coating was then applied to the other side (A-grade side).

Each coated plywood panel was cut into 121 specimens that measured 4 in. x 8 in. (102 mm x 204 mm), providing a total of 363 specimens. Specimens from the three plywood panels were sequentially numbered 1-121 (Panel 1), 122-242 (Panel 2), and 243-363 (Panel 3). Figure 1 shows a cut pattern for a single plywood panel with 121 specimens. In addition to the discarded edge sections, specimens from the left and top edges of the panels were also discarded to avoid cracked or split edges that may have existed prior to cutting, leaving a total of 100 available specimens per panel.

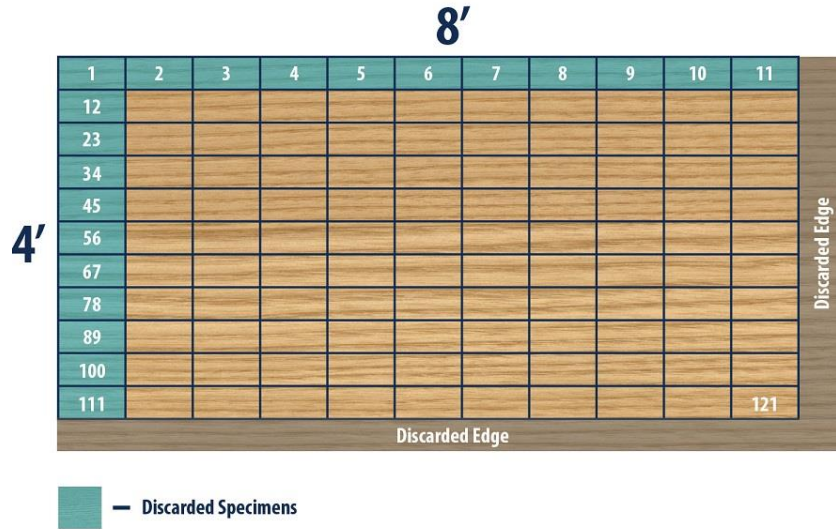


Figure 1. Cut pattern for plywood panel specimens. Note: Panel edges on right and bottom were discarded, and specimens aligned to left and top edges were not used.

Experimental factors for testing of the products included outdoor weathering periods (0, 3, 6, 12, 18, 24, 36, 48, and 60 months), outdoor weathering exposure (north or south orientation), and different levels of radiant heat exposure (30, 50, or 70 kW/m²). For each of the five coatings, a given 4-in. x 8-in. (102-mm x 204-mm) specimen was randomly allocated to a treatment combination (i.e., weathering period, exposure, and radiant heat level). Each of these treatment combinations was replicated three times for each panel, making a total of nine samples for each treatment combination. Refer to Table 1 for a summary of the experimental design factors.

Table 1. Experimental design factors.

Factor	Description
Coating	A, B, C, D, E
Weathering period	0, 3, 6, 12, 18, 24, 36, 48, 60 months
Weathering orientation	North, south
Radiant heat exposure	30, 50, 70 kW/m ²
Replications	3

Natural Weathering

The specimens to be weathered were placed on an aluminum fence located at the IBHS Research Center. The capacity of the test fence was 1,232 specimens. Half of the specimens were placed on the north-facing side and the other half were placed on the south-facing side. Photographs and diagrams of the fence are shown in Figure 2. In addition to a control specimen (0 months and no weathering), each coating had

specimens that were subjected to multiple weathering periods as shown in Table 2. This report includes only those results from the first 12 months of the study.



Figure 2. Specimens on the weathering fence (top), and the weathering fence at noon (bottom) with northern exposure on the left and southern exposure on the right (Bahrani, 2015).

Table 2. Weathering periods and scheduled removal from weathering fence.

Weathering Period	Scheduled Removal from Weathering Fence
0-Month	January 2015
3-Month	April 2015
6-Month	July 2015
12-Month	January 2016
18-Month	July 2016
24-Month	January 2017
36-Month	January 2018
48-Month	January 2019
60-Month	January 2020

Environmental conditions at the IBHS Research Center were recorded at a weather station located approximately 1,100 ft (330 m) east of the weathering fence. Data was collected for conditions including wind speed and direction, measured at 33 ft (10 m); temperature, measured at 30 ft (9 m); relative humidity, measured at 6.6 ft (2 m); barometric pressure; precipitation; and total incoming solar radiation measured on a panel having a 6:12 slope for both a northern and southern exposure. All environmental data was based on 5-minute averages.

After removing the specimens from the fence, they were cut in half to produce two 4-in. x 4-in. (100-mm x 100-mm) squares. One of the squares for each specimen was delivered to UNC Charlotte for combustibility tests. The other square was kept at IBHS for the surface evaluation and paint film thickness measurements.

Surface Evaluation

The specimens used for surface evaluation were randomly selected and visually examined for changes after each weathering period. This was done by IBHS staff. The surface of each coated specimen for the different weathering periods and orientations was documented in photographs. Several features were noted, including cracking of the coating, loss of gloss, flaking of the coating, discoloration, and mold growth.

There was a total of 24 specimens for each coating and weathering period, 12 being a northern exposure and 12 being a southern exposure. For each group of 12 exposures, four specimens came from each of the three panels. Due to the large number of specimens then, only three from each exposure group were selected, one from each panel.

Combustibility Tests

The cone calorimeter combustibility tests were conducted in accordance with the American Society for Testing and Materials (ASTM), specifically ASTM E1354-15 (2015). Specimens were positioned horizontally under a cone heater and subjected to one of three radiant heat fluxes used in this study. A spark igniter positioned at 1 in. (25 mm) below the cone was used as a pilot for ignition. (Refer to Figure 3.) Exposure levels included 30, 50, and 70 kW/m², which are common levels representing low-, medium- and high-level exposures, respectively (Schartel and Hull, 2007). Use of the different exposure levels provided information on response time for the intumescent or fire-retardant products. These products need to be responsive over a wide range of exposures if they are to provide effective protection to a building. All tests were recorded using two video cameras, one horizontally positioned in front of the specimen and the other at a 45-degree angle to the specimen. The cameras recorded the growth of the intumescent coating (Bahrani, 2015). The videos were then used to obtain the expansion ratio and the maximum height of the intumescence for each specimen via second-by-second image processing using the matrix laboratory (MATLAB) numerical computing program. At the beginning of a given test, a digital thermo-hygrometer was used to measure ambient temperature, ambient pressure, and relative humidity.

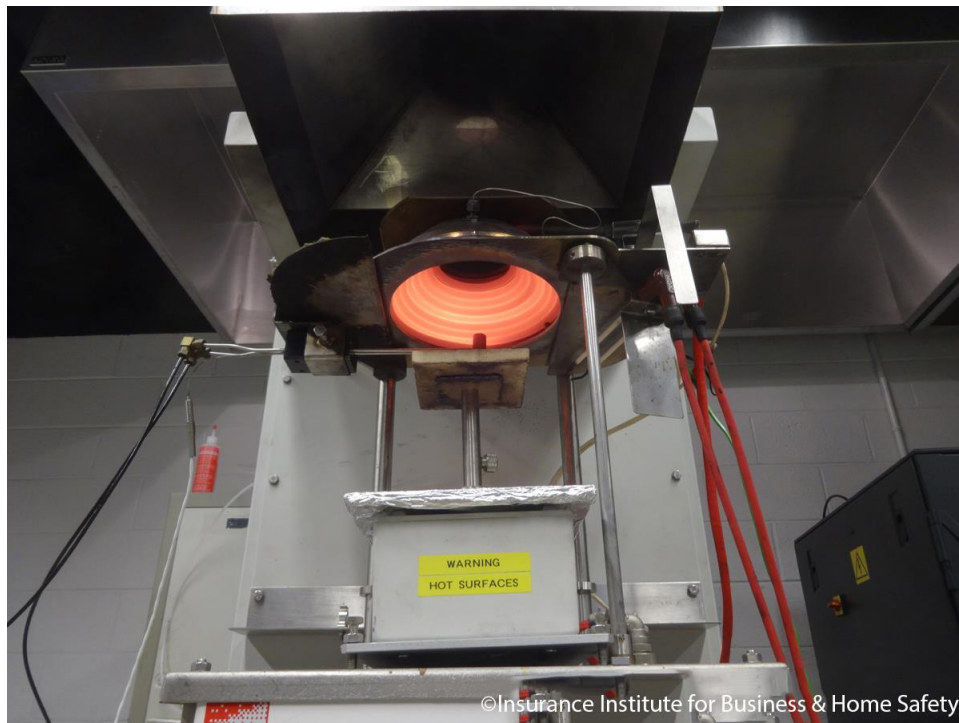


Figure 3. Cone calorimeter conical heater component. The specimen is positioned on the raised platform located below the heater component.

Three replicates were tested at each heat flux level for each coating and for a given weathering period and orientation. Data collected for the heat release rate (HRR) was gathered at one-, three-, and five-minute periods. Since some of the combustibility tests were completed prior to five minutes, the data collected at three minutes was used to analyze and plot the HRR diagrams (Bahrani, 2015).

Time to ignition (TTI), time to intumescence (Tintu), and peak heat release rate (PHRR) will be discussed in this report. The TTI indicated the amount of time it took for ignition of the specimen to occur, whereas Tintu corresponded to the time it took for the specimen to form intumescence. The PHRR indicated the amount of heat released by the burning specimen. Evaluation and measurements of the coating (i.e., Tintu) allowed for comparisons of coating performance (Wang et al., 2005). Mean values for the cone calorimeter tests for each film-forming coating are provided in Appendix A.

Measurement of Paint Film Thickness

To evaluate the influence of paint film thickness on fire performance, thickness was measured before weathering and after each weathering period. Penetrants D and E were not included as they did not form a film. The natural color of the penetrants also made it difficult to measure penetration depth. For Coatings A, B, and C, the paint film thickness was measured following the guidelines provided in ASTM D5235-14 (2014). Each of the selected 4-in. x 4-in. (100-mm x 100-mm) specimens was cut into two 2-in. x 4-in. (50-mm x 100-mm) pieces. One piece was saved for future evaluation and the other was further cut into four equally sized pieces measuring 1-in. x 2-in. (25-mm x 50-mm). Refer to Figure 4. These pieces were labeled 1A, 1B, 2A, and 2B. The 1A and 1B pieces were face-glued together, using a clear hot-melt adhesive, to create a 1-in. x 2-in. block with a thickness that was twice the panel thickness. The same procedure was followed for the 2A and 2B pieces. This procedure resulted in two samples that were used to determine paint film thickness.

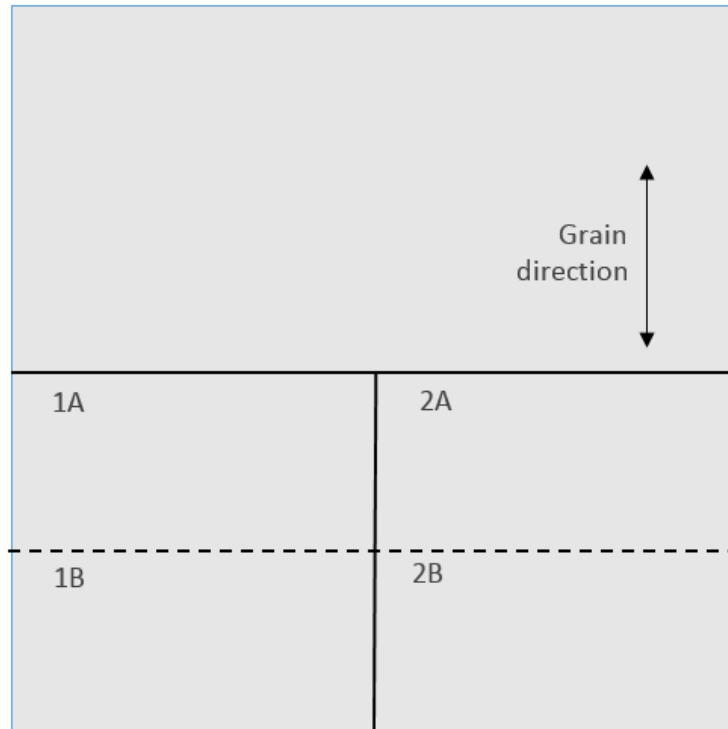


Figure 4. Specimen preparation for measuring film thickness.

Once the pieces were face-glued together, the surfaces of the samples were prepared for measurement of paint film thickness as specified in ASTM D5235-14 (2014). Both long edges of the samples were sanded using a 200-grit sandpaper. To finish preparation, the samples were sanded again using a 600-grit sandpaper. Each long edge was then divided into four 0.5-in. (12.5-mm) sections for measurement as shown in Figure 5. Each of the samples selected for thickness measurements were prepared in this manner.



Figure 5. Prepared samples (top) with sanded edges (B side shown), and sample (bottom) divided into four sections (A side shown) for measuring paint film thickness.

The paint film thickness of each sample was determined using a microscope with a 3.2x magnification. Using the manufacturer provided software that determined the distance between the two specified points, the paint film thickness was measured, as shown in Figure 6. The paint film was measured in each of the four sections, both above and below the glued surface and on each long edge of the sample. The location of the two measurements in each of the four sections was arbitrary but was typically at the midpoint of each section.

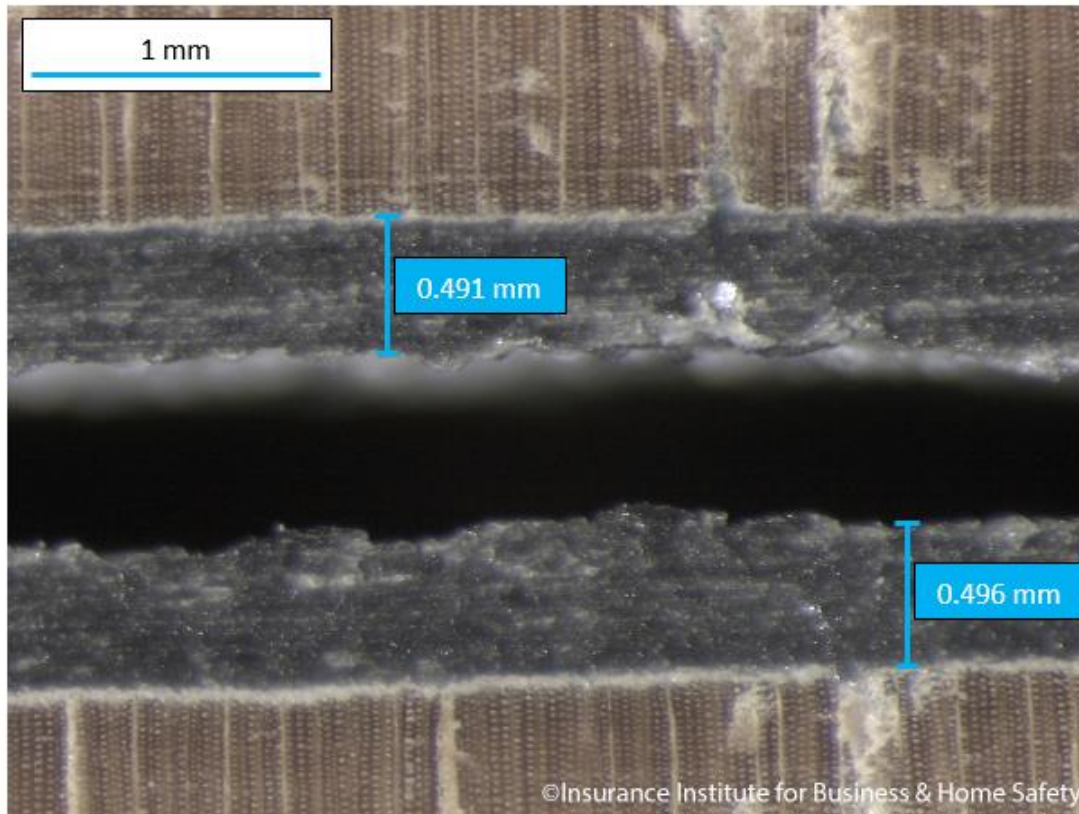


Figure 6. Example of paint film thickness measurements along the glued interface between coated pieces. Note: 1 mm = 0.039 in.

Results and Discussion

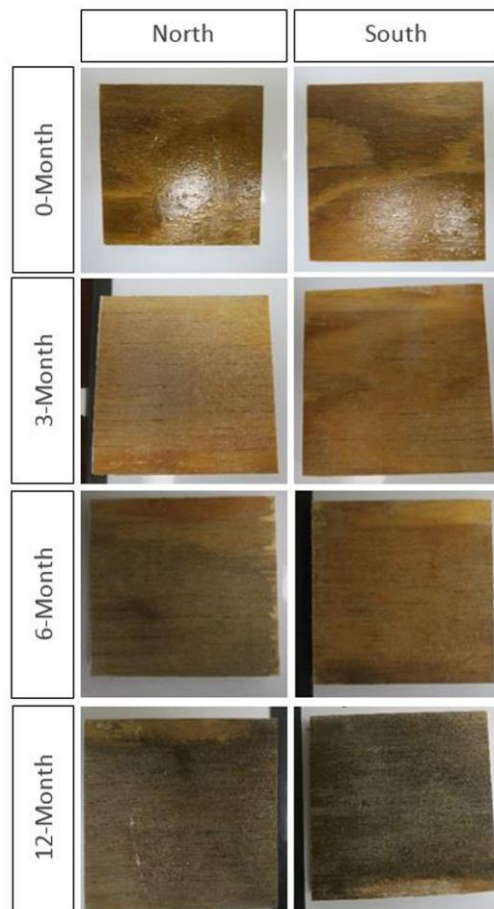
The detailed results for the surface evaluation, combustibility tests, and paint film thickness measurements are discussed in this section. When applicable, bar graphs were created to show the changes in the mean value for orientation and weathering. All bar graphs include an estimated uncertainty of plus or minus one standard deviation.

Surface Evaluation

The surface evaluation portion of the analysis included a qualitative discussion of the appearance of the coatings or substrate (when applicable). A diminished performance of the coating could result from a reduction in coating thickness, development of cracks or other voids in the coating due to dimensional changes in the coating and/or substrate, and other chemical changes (not measured) in the coating. A surface evaluation was conducted to understand these potential causes of change in the measured fire properties.

Film-Forming Coating A

The degradation of Coating A specimens as a function of weathering period and orientation is shown in Figure 7. This was initially a glossy, clear coating. After the 3-month weathering period, both the north and south oriented specimens experienced notable loss of gloss. Long cracks, typically referred to as surface checks, also developed along the grain. Of the six specimens evaluated, flaking of the coating was observed on two north oriented specimens. After the 6-month weathering period, continued loss of gloss and surface checks were observed on the specimens. Mold growth on the surface was also visible. After the 12-month weathering period, the specimens exhibited additional discoloration that resulted from continued mold growth. No evidence of gloss remained. There were several specimens where the coating had flaked off over a large area. There was no observable difference in the surface characteristics between the north and south oriented specimens after all weathering periods.



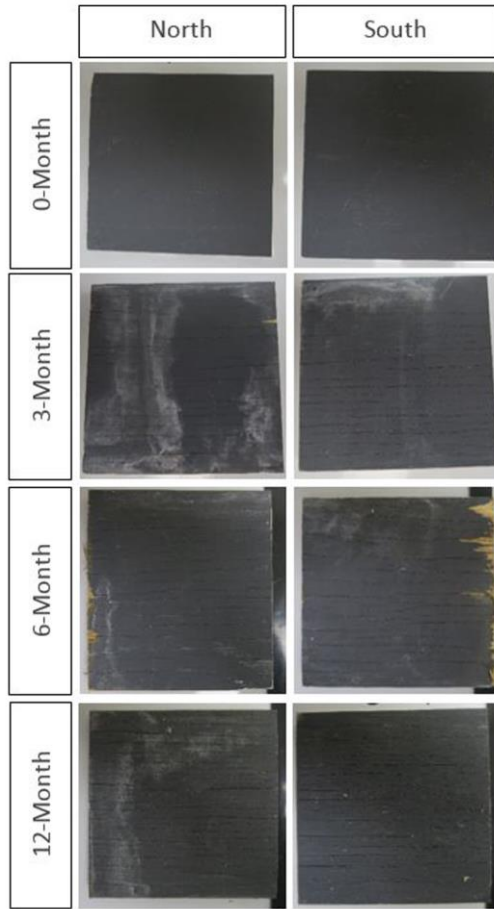
©Insurance Institute for Business & Home Safety

Figure 7. Qualitative surface evaluation of Coating A specimens as a function of weathering period and orientation.

Film-Forming Coating B

The degradation of Coating B specimens as a function of weathering period and orientation is shown in Figure 8. This was a pigmented coating. After the 3-month weathering period, both the north and south oriented specimens exhibited surface checks. For one of the specimens, the cracking was deep enough to expose the substrate beneath the coating. In addition to the surface checks, the coating also began to exhibit a white, chalky appearance. After the 6-month weathering period, surface checks were still prevalent. The south oriented specimen appeared to experience more severe degradation given the presence of deeper checks and some flaking of the coating. There was still a white, chalky appearance as seen with the 3-month weathering period. It should be noted that surface checks observed along the edge of the 6-month specimens, as shown in Figure 8, were caused by the band saw cut and not related to weathering.

No differences were observed between the 6- and 12-month, north oriented specimens. For these weathering periods, surface checks were prevalent. For the south oriented specimens, however, all experienced flaking of the coating that exposed the substrate. When the specimens were removed from the fence, care was taken to prevent loss of the coating due to the noticeable flaking.

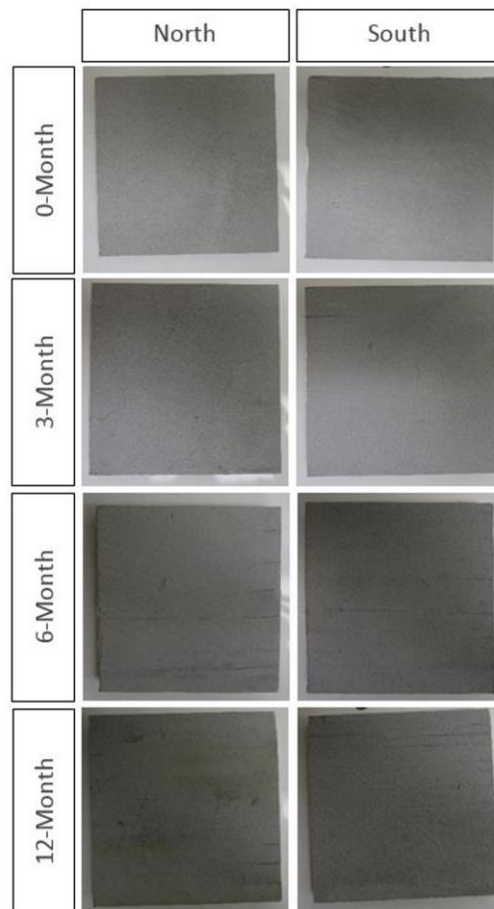


©Insurance Institute for Business & Home Safety

Figure 8. Qualitative surface evaluation of Coating B specimens as a function of weathering period and orientation. Note: Cracks in the 6-month specimens resulted from cutting with a band saw, not weathering.

Film-Forming Coating C

The degradation of Coating C specimens as a function of weathering period and orientation is shown in Figure 9. This coating was pigmented. After the 3-month weathering period, no surface checks were observed on the north oriented specimens. However, two of the three south oriented specimens had developed surface checks that were approximately 0.8 to 1.6 in. (20 to 40 mm) in length. After the 6-month weathering period, several specimens had developed surface checks that spanned their entire length. No noticeable discoloration or mold growth was observed on these specimens. After the 12-month weathering period, three of the six specimens had numerous surface checks along their entire length. The specimens that exhibited only minor surface checks were those with a north orientation. The north oriented specimens also began to experience discoloration and mold. Of the coatings evaluated in this study, Coating C performed best in terms of resisting development of checks, discoloration, and mold.



©Insurance Institute for Business & Home Safety

Figure 9. Qualitative surface evaluation of Coating C specimens as a function of weathering period and orientation.

Penetrant Coating D

The degradation of Coating D specimens as a function of weathering period and orientation is shown in Figure 10. After the 3-month weathering period, surface checks were observed on all six specimens. Some of these checks spanned the entire length of the specimen. Mold growth was observed on one north oriented specimen. After the 6-month weathering period, the specimens had long, deep surface checks along the grain. Mold growth was observed on five of the six specimens. The extent of the surface checks increased during the 6- to 12-month weathering period. The discoloration of the substrate was also more noticeable. It appeared that the three south oriented specimens experienced more weathering than the three north oriented specimens.

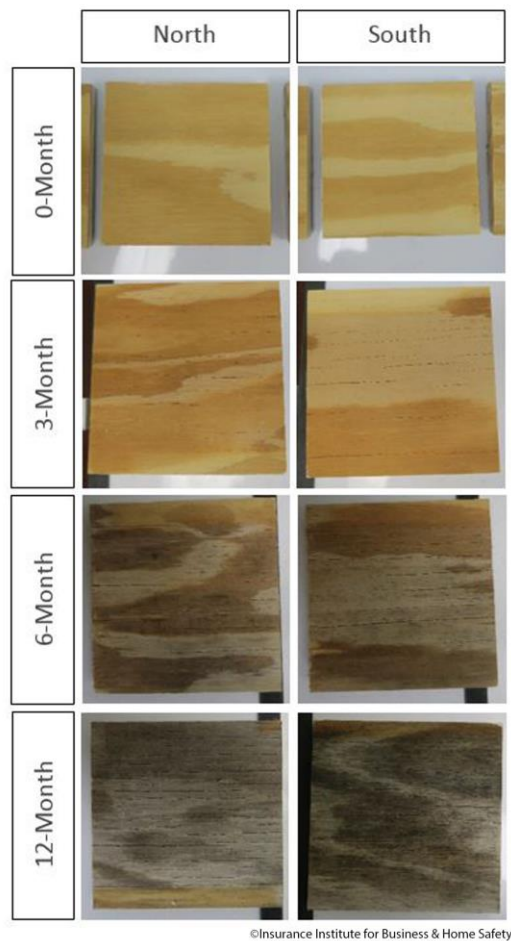


Figure 10. Qualitative surface evaluation of Coating D specimens as a function of weathering period and orientation.

Penetrant Coating E

The degradation of Coating E specimens as a function of weathering period and orientation is shown in Figure 11. This coating was initially a glossy, clear coating. After the 3-month weathering period, the north and south oriented specimens exhibited surface checks and mold growth. After the 6-month weathering period, longer cracks were observed and mold growth appeared over a larger area. Like Penetrant D, a discoloration of the substrate was also more noticeable following the 6- to 12-month weathering period. There were no differences observed between the north and south oriented specimens.

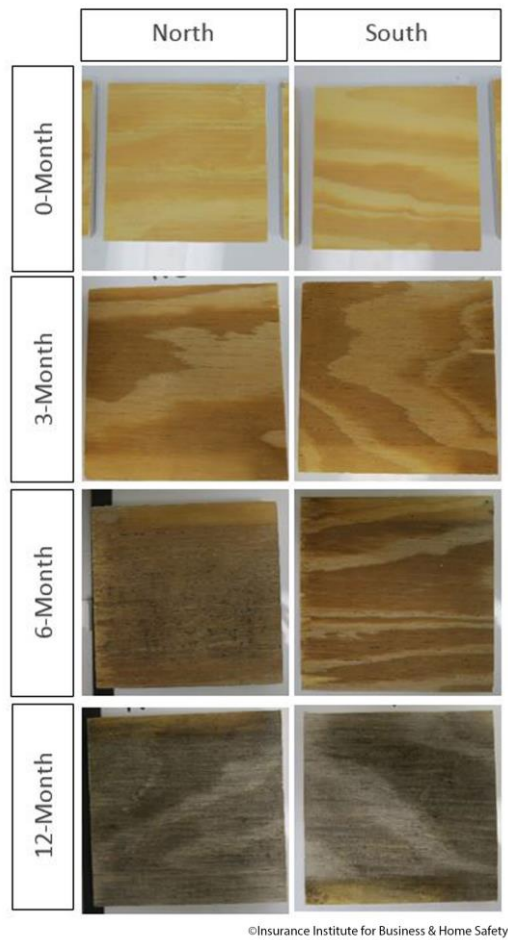


Figure 11. Qualitative surface evaluation of Coating E specimens as a function of weathering period and orientation.

Summary of Surface Evaluation

Development of surface checks occurred in some specimens as early as the 3-month weathering period. Surface checks that penetrated the coating could have negative impact on performance of the coating.

Loss of gloss in the clear Coating A occurred during the initial 3-month weathering period. Mold growth was common as weathering time increased, but typically present after the 6-month weathering period. Differences in exposure (north and south) were minimal.

Combustibility Tests

Only select combustibility properties were measured for each coating. The performance of the coating products was determined by (1) comparing the coated and weathered specimens to uncoated and non-weathered specimens and (2) assessing any degradation of performance for a given coating product as a function of weathering. The TTI and PHRR data for an uncoated and non-weathered specimen is shown in Table 3. Note that the TTI decreased and PHRR increased with exposure to increasing radiant heat flux levels.

Table 3. Summary of cone calorimeter results for uncoated, non-weathered specimen (Bahrani, 2015).

Heat Flux Level (kW/m ²)	TTI (s)	PHRR (kW/m ²)
30	75	225
50	20	329
70	12	339

Limited combustibility data was included for Penetrants D and E. Only TTI and PHRR for 0- and 12-month weathering will be discussed. Results for Coatings A, B, and C will include TTI, T_{intu} , and PHRR data.

In evaluating these coatings, higher values for TTI, shorter values for T_{intu} , and lower values for PHRR were indicative of better coating performance. TTI values could be compared to the uncoated controls. An effective service life was evaluated based on a comparison of the coating performance after weathering to the coating performance in a non-weathered, uncoated state. TTI was the most important criteria in evaluating coating performance, followed by PHRR. T_{intu} was used to understand response times to different radiant heat exposure levels. Given the inability to predict the exposure that will be most critical when a wildfire threatens, a conservative approach would be to associate effective service life with the shortest weathering period where coated specimens outperformed uncoated specimens.

Some of the bar charts in this section include error bars representing uncertainty of plus or minus one standard deviation. Results for each product will be discussed and summarized in this section.

Film-Forming Coating A

In the non-weathered (0-month) condition, Coating A performed better than the uncoated control when evaluated based on two of the performance measures (TTI and PHRR). A comparison of T_{intu} cannot be made with the uncoated control. For the north and south oriented specimens, the observed performance trends were similar, and any differences in performance were minimal. TTI was consistently longer for the 30 kW/m² heat flux level compared to the 50 and 70 kW/m², at each weathering period.

TTI results for Coating A are shown in Figure 12. Comparing TTI for the non-weathered uncoated and coated specimens indicated that Coating A outperformed the uncoated specimen, especially at the 30 kW/m² level, where the average TTI was delayed by over 3.5 minutes (210 seconds). The relative improvement in TTI was less at the 50 and 70 kW/m² exposure levels. At these higher heat flux levels, the average increase in TTI was 49 and 27 seconds, respectively. Comparing performance for each heat flux exposure level, results indicated that the northern exposure was slightly more severe than the southern exposure. For the south oriented specimens, though differences were small, there was a slight performance advantage for coated samples at the 50 and 70 kW/m² radiant heat levels.

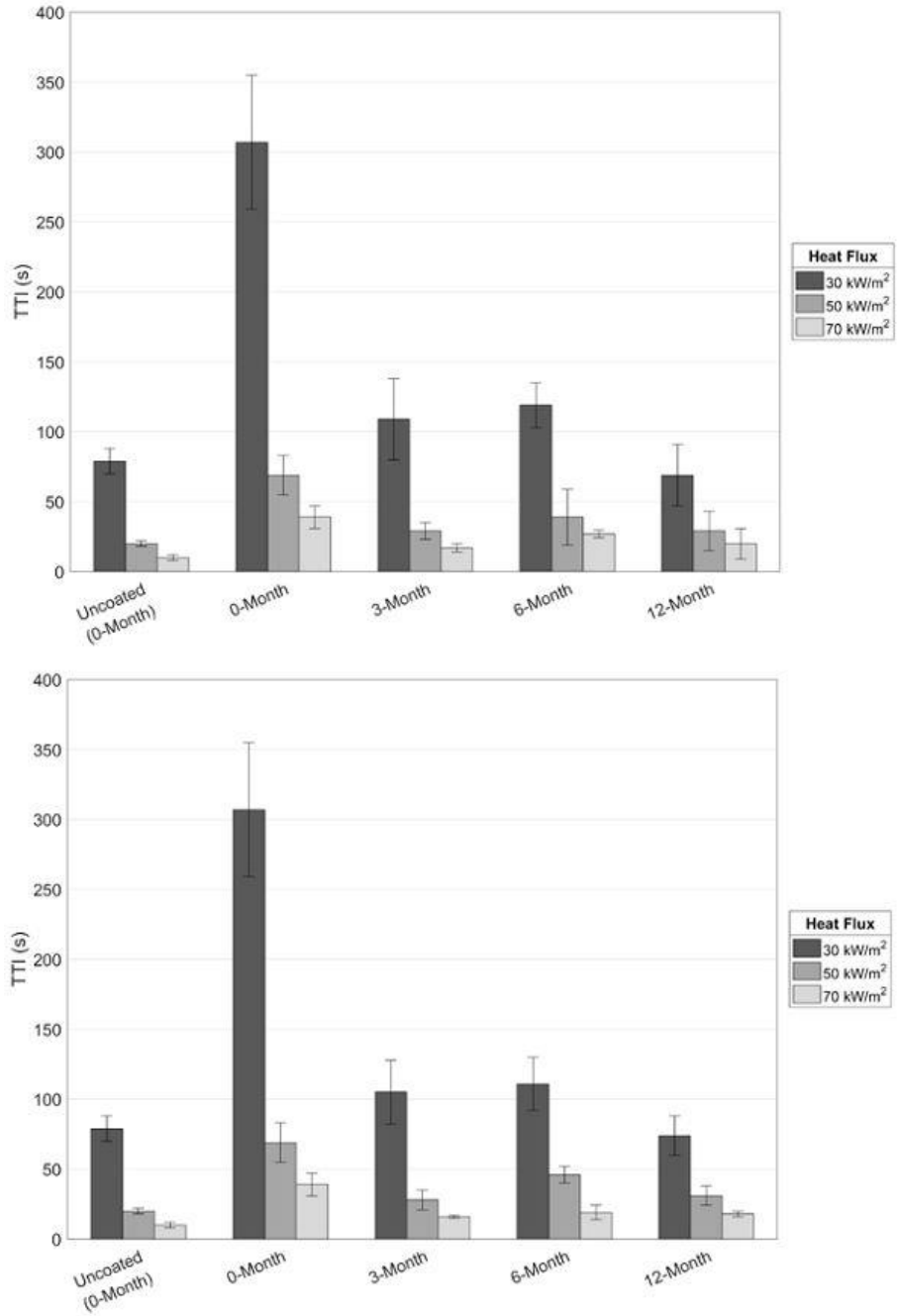


Figure 12. TTI as a function of weathering for Coating A with northern exposure (top) and southern exposure (bottom).

T_{intu} results for Coating A are shown in Figure 13. Comparing non-weathered and weathered results, T_{intu} was noticeably longer at the lowest heat flux level. Differences were less dramatic at the 50 and 70 kW/m² heat flux levels. At the 0-month weathering period, it took a little over 20 seconds for the intumescence layer to form. After the 3-month weathering period, the time to form intumescence nearly tripled, indicating a reduction in the protective performance of the coating. After three months, T_{intu} remained relatively constant, regardless of the heat flux level. No difference was observed between the north and south oriented specimens.

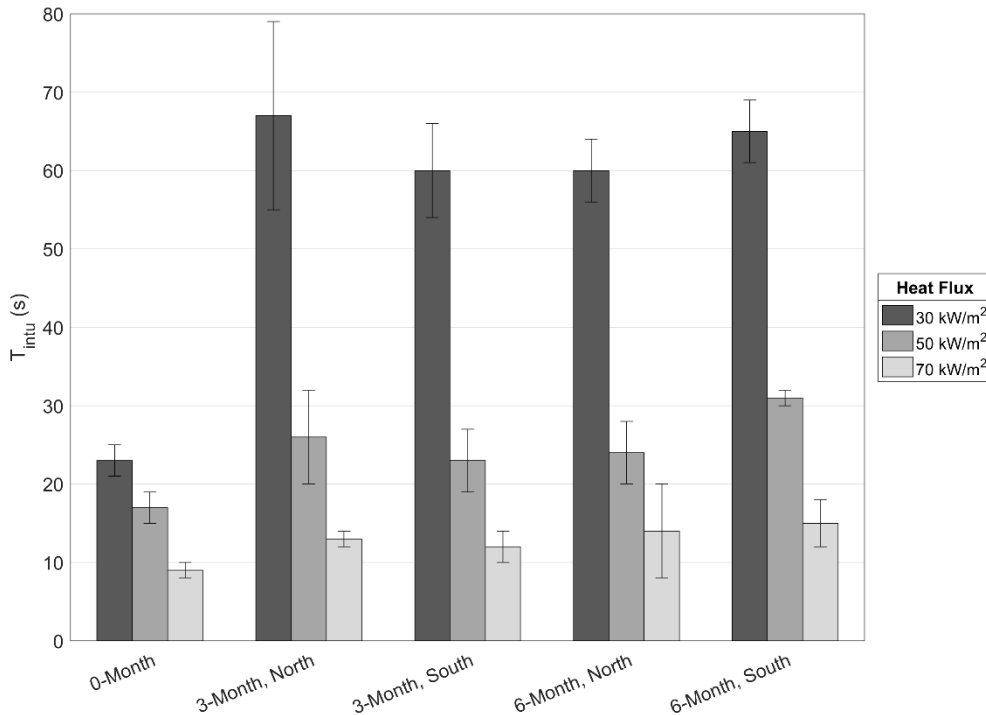


Figure 13. T_{intu} for Coating A.

PHRR results for Coating A are shown in Figure 14. For coated and uncoated specimens, the PHRR consistently increased with the increased heat flux levels. The PHRR for coated specimens was lower than that for the uncoated specimens, indicating the coating was performing as desired. For the north oriented specimens, no difference between coated and uncoated was observed after the 3-month weathering period. A similar result was observed at the 30 kW/m² heat flux level for the south oriented specimens. PHRR results for the 50 and 70 kW/m² heat flux levels were less uniform than at the 30 kW/m² level, but the general trend was the same.

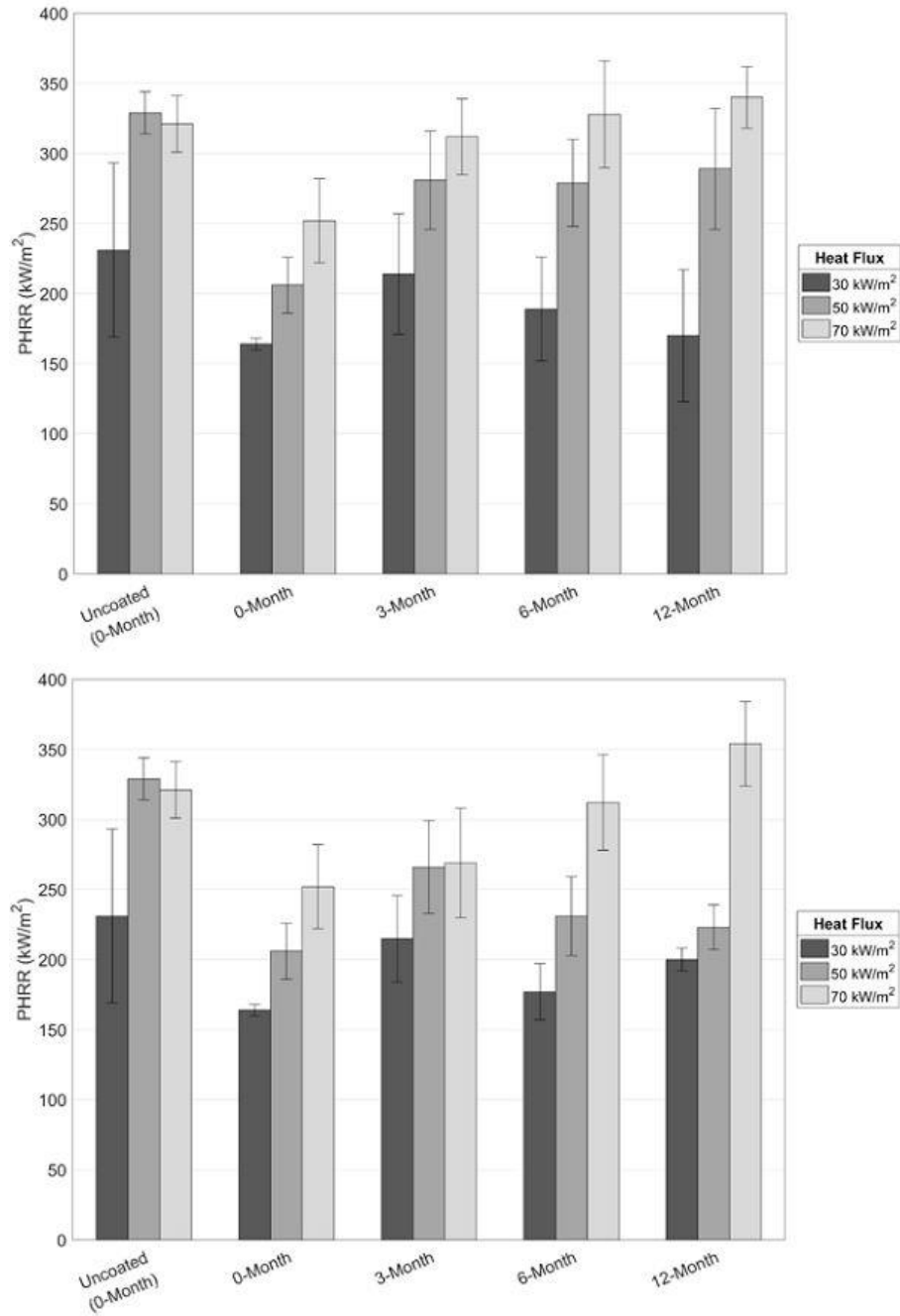


Figure 14. PHRR as a function of weathering for Coating A with northern exposure (top) and southern exposure (bottom).

Film-Forming Coating B

TTI results for Coating B are shown in Figure 15. Comparing TTI for the non-weathered uncoated and coated specimens showed that ignition of the Coating B specimen was delayed by over seven minutes at the 30 kW/m² heat flux level. The reduction in TTI was very small at the higher heat flux levels (6 seconds for 50 kW/m² and 12 seconds for 70 kW/m²). This indicated inconsistent protection, particularly at moderate to high heat flux levels.

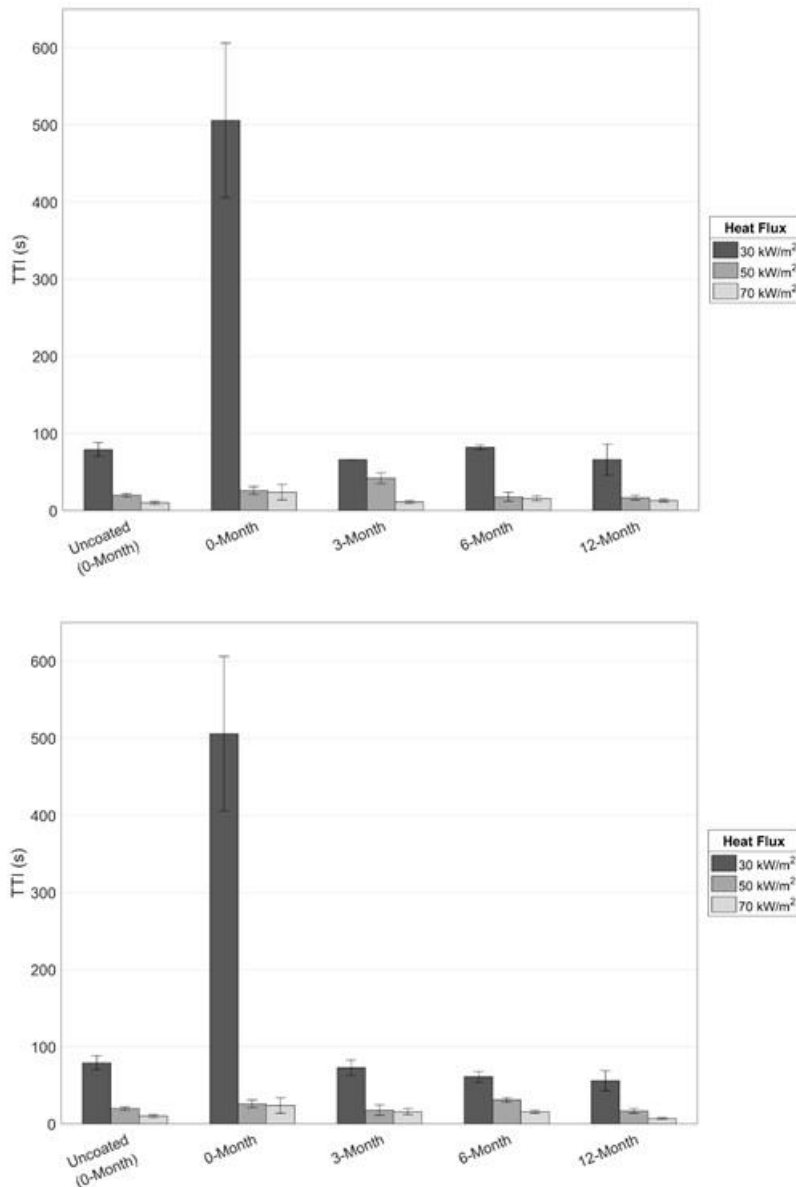


Figure 15. TTI as a function of weathering for Coating B with northern exposure (top) and southern exposure (bottom).

At the 30 kW/m² heat flux level, there was an 85 percent decrease in TTI after three months of weathering for both the north and south oriented specimens. After three months, TTI at the 30 kW/m² exposure level remained relatively constant. Results for the north and south oriented specimens were similar, indicating no difference in performance as a function of exposure.

T_{intu} results for Coating B are shown in Figure 16. The intumescence was observed at the 0- month period for tests at all three heat flux levels. After the 3-month weathering period, intumescence was only observed with the north oriented specimen tested at the 50 kW/m² heat flux level. These results indicated that even short-term weathering had a negative impact on the activation of the coating.

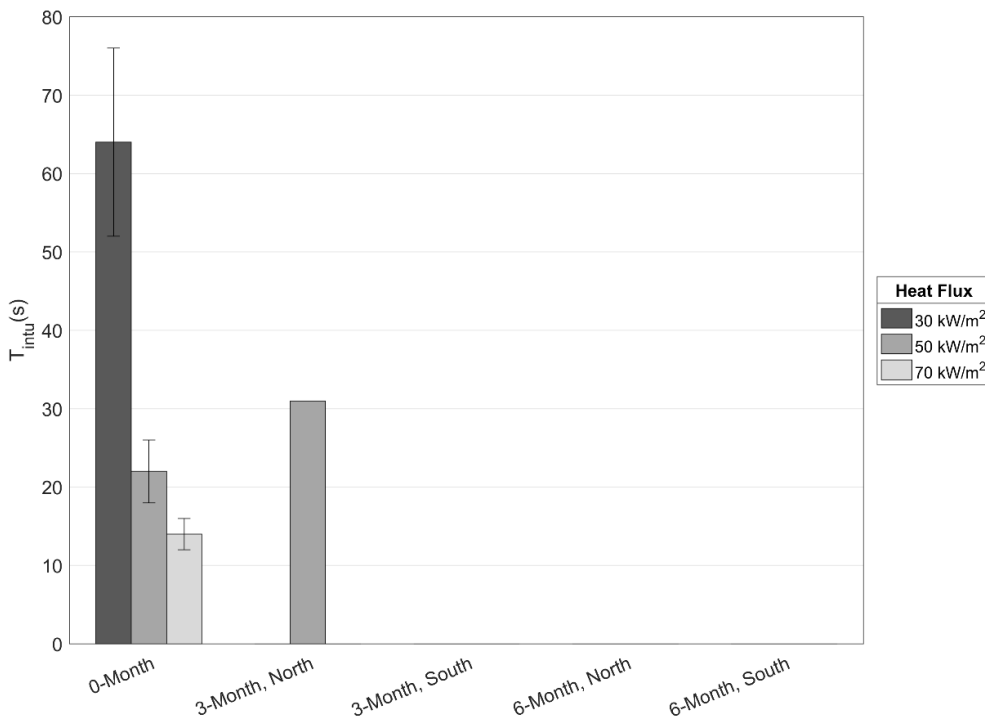


Figure 16. T_{intu} for Coating B.

PHRR results for Coating B are shown in Figure 17. Results for the north and south oriented specimens were similar, each showing that differences between the non-weathered uncoated and coated specimens were minimal. Improvement in performance was only observed for tests conducted at the 50 kW/m² heat flux exposure level.

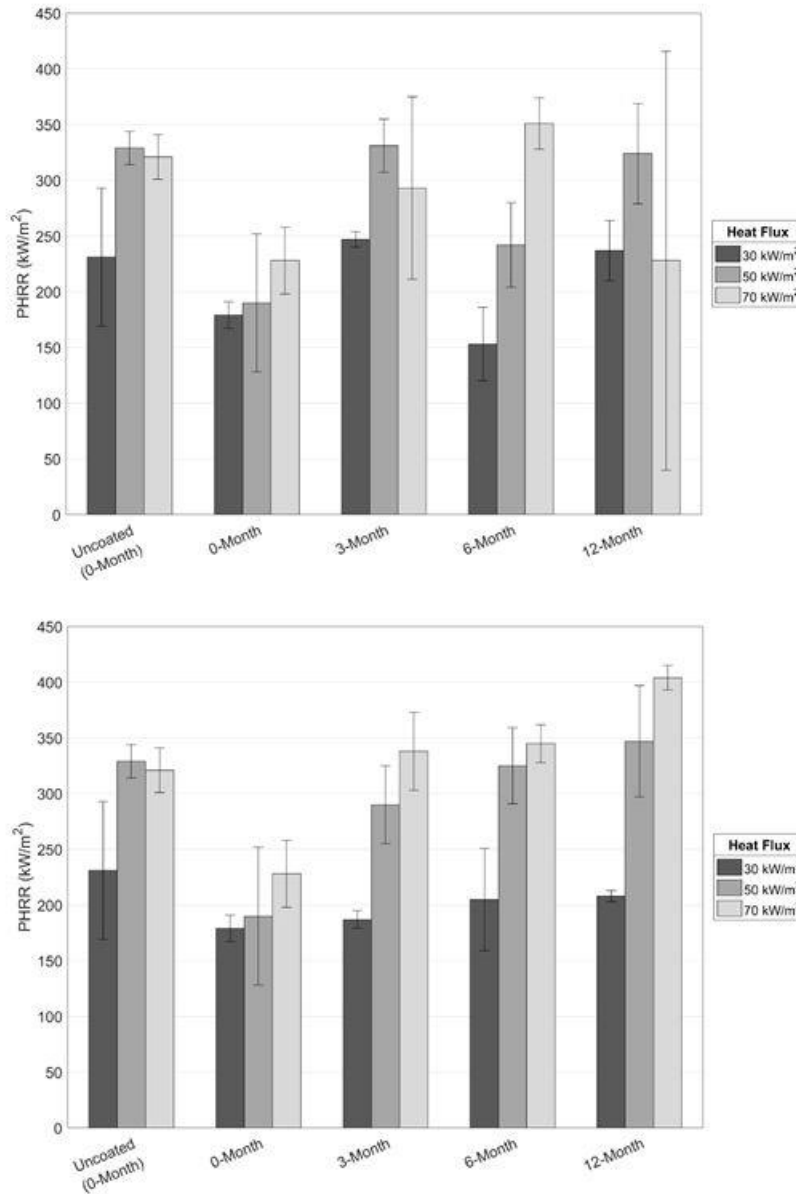


Figure 17. PHRR as a function of weathering for Coating B with northern exposure (top) and southern exposure (bottom).

Film-Forming Coating C

TTI results for Coating C are shown in Figure 18. The north and south oriented specimens performed similarly at all weathering periods and heat flux exposure levels. At the lower heat flux exposure levels (30 and 50 kW/m²), coated specimens performed better than uncoated controls. No difference was observed between coated and uncoated specimens when tested at the highest heat flux level (70 kW/m²). The observed difference in response to heat flux exposure levels indicated that there was likely a limit to which the coating provided protection.

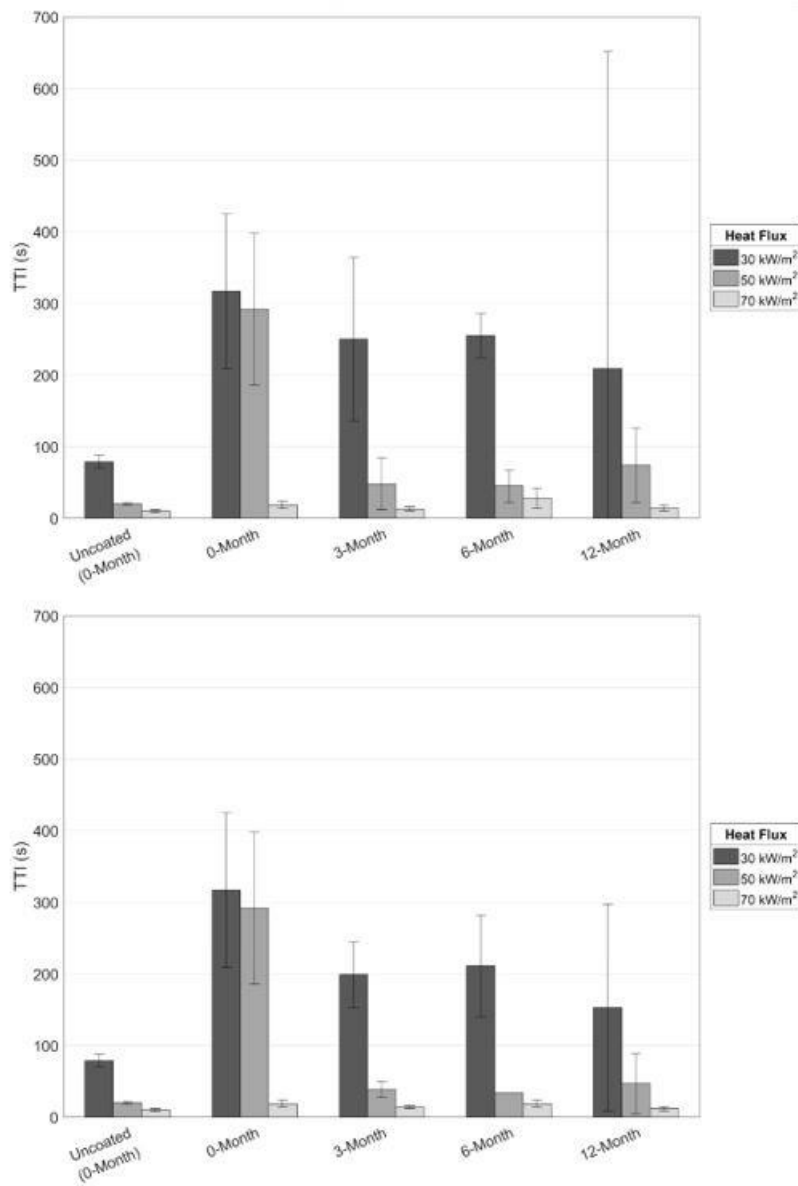


Figure 18. TTI as a function of weathering for Coating C with northern exposure (top) and southern exposure (bottom).

T_{intu} results for Coating C are shown in Figure 19. Differences in T_{intu} for the different weathering periods were minimal at the low and high heat flux levels. At the middle heat flux level, T_{intu} decreased after the first weathering period but remained constant thereafter. Differences in T_{intu} for the north and south oriented specimens were small and not consistent.

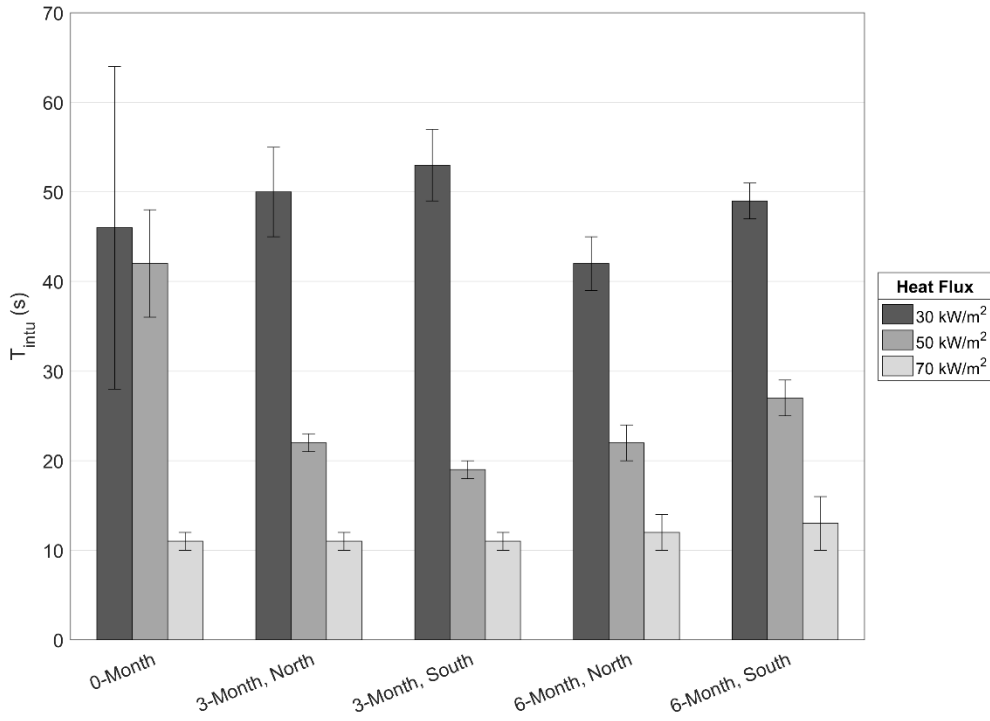


Figure 19. T_{intu} for Coating C.

PHRR results for Coating C are shown in Figure 20. PHRR for the coated non-weathered specimens was consistently lower than the uncoated controls. For the north oriented specimens, this trend continued through the 12-month weathering period. The same trend was apparent for the south oriented specimens at the 30 and 50 kW/m² heat flux exposure levels, and performance of the coated specimens exceeded that of the uncoated controls through the 12-month weathering period. For the south oriented specimens, no differences were observed between coated and uncoated control specimens tested at the highest heat flux level (70 kW/m²).

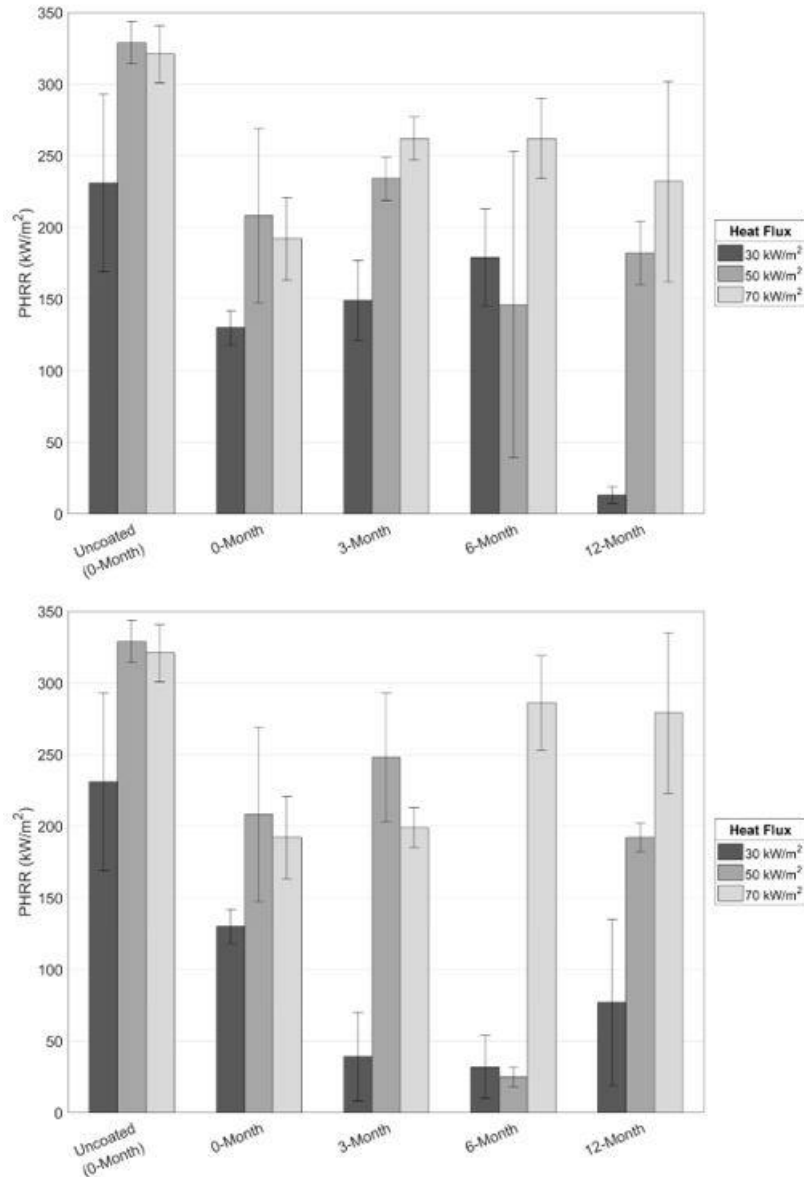


Figure 20. PHRR as a function of weathering for Coating C with northern exposure (top) and southern exposure (bottom).

Penetrant Coatings D and E

For the penetrant coatings, cone calorimeter data was analyzed for the 0- (control) and 12-month weathering periods. TTI and PHRR results are shown in Figures 21 and 22, respectively. The plotted data shows averages of measurements taken for north and south oriented specimens. Differences in performance for TTI decreased with increased exposure levels. At the 30 kW/m² radiant heat exposure level, the uncoated and non-weathered specimen performed better than the coated specimens (i.e., the TTI was longer). Differences in performance as a function of weathering and coating were not apparent at the 50 and 70 kW/m² exposure levels.

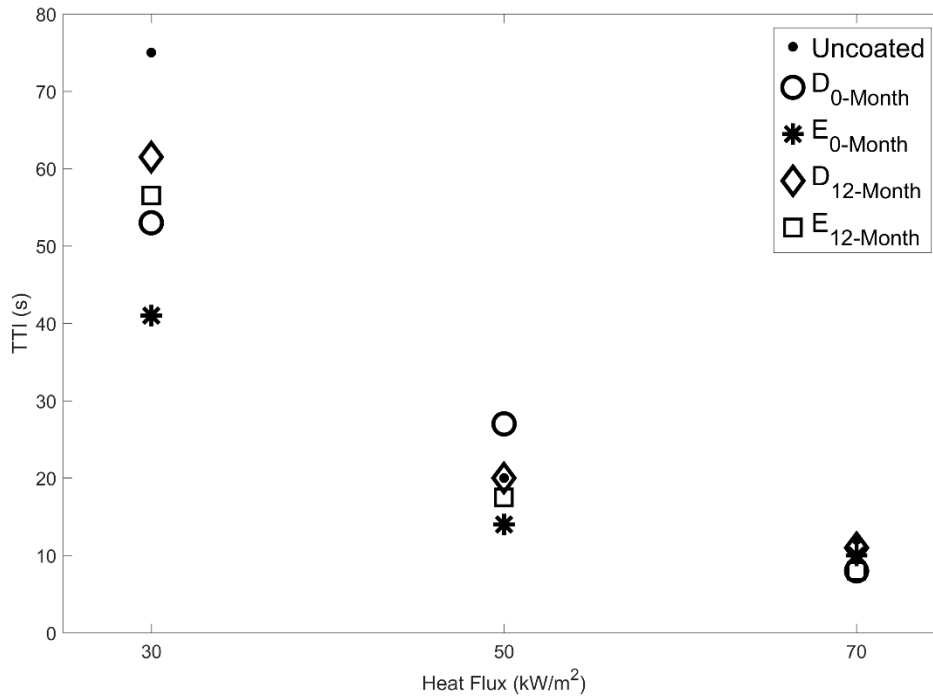


Figure 21. TTI data for Coatings D and E after 0- and 12-month weathering periods. Results for the uncoated and non-weathered control are also shown.

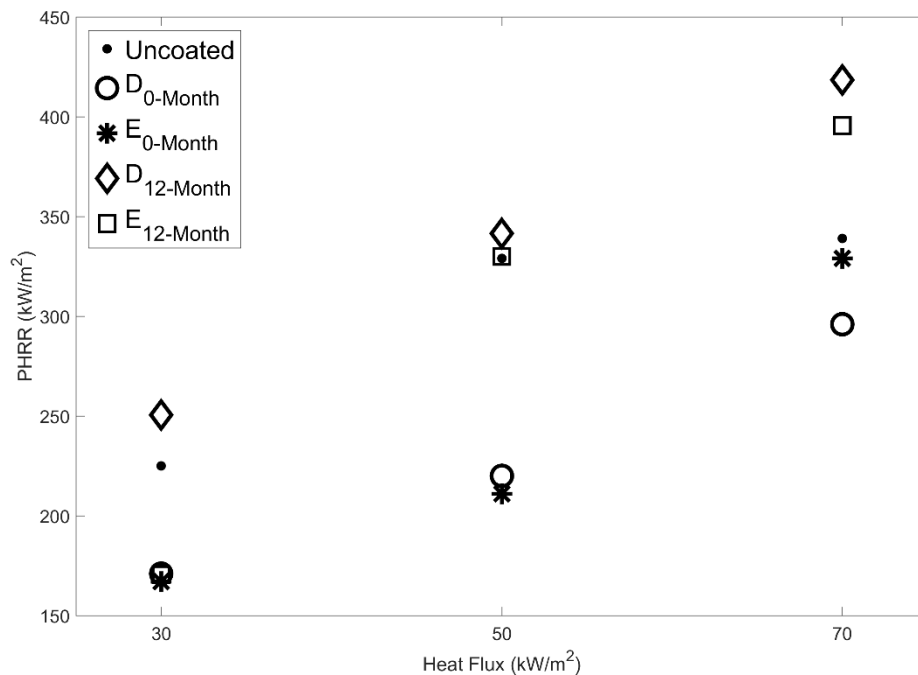


Figure 22. PHRR data for Coatings D and E after 0- and 12-month weathering periods. Results for the uncoated and non-weathered control are also shown.

Results of the PHRR data for Coatings D and E were similar in that the uncoated, non-weathered specimen result was typically between the coated, weathered specimen results. At the 50 and 70 kW/m² heat exposure levels, weathering resulted in a higher PHRR for the penetrant products. Results for the penetrant with non-intumescent characteristics were like those for the intumescent product. Because of the poor performance of the penetrant products, particularly when considering TTI, additional testing was not conducted.

Summary of Combustibility Tests

As previously stated, TTI was considered the most important criteria in evaluating coating performance. A summary of the TTI results for each coating is shown in Figures 23 through 25. Each figure shows the average values for the weathering periods at each radiant heat exposure level. The error bars represent a measure of variability. The average values for the uncoated specimens are indicated by a horizontal line at one standard deviation. Data for the coated specimens were compared to these values.

The TTI data was analyzed using an analysis of variance (ANOVA) procedure. This analysis indicated that there was no significant difference between the northern and southern exposures ($\alpha = 0.05$). Therefore, these data were combined to make the summary plots shown in Figures 23 through 25.

Each of these plots showed that the coatings for non-weathered specimens generally performed better than the uncoated specimens and that coating performance increased with tests conducted at the lowest (30 kW/m²) heat flux level. Performance results for the coatings were poor when coated specimens were tested at the higher (50 and 70 kW/m²) heat flux levels. Results also clearly showed that even in cases where non-weathered and coated specimens performed better than weathered and coated specimens, there was a dramatic reduction in performance after the 3-month weathering period.

For comparison purposes, the coatings were judged to have an adequate performance if the average TTI value for the coating product, minus one standard deviation, was greater than the average TTI value of the uncoated control, plus one standard deviation:

$$\text{Adequate Performance if } [\mu_{TTI_{coated}} - \sigma_{coated}] > [\mu_{TTI_{uncoated}} + \sigma_{uncoated}]$$

where μ indicates the mean and σ indicates the standard deviation.

As shown in Figures 23 through 25, when all heat flux exposure levels are considered and regardless of the weathering period, none of the coating products provided significant protection when coated specimens were compared to the uncoated specimens. At least with current formulations, these coating products cannot be relied on to provide any enhanced protection for radiant heat exposures over an uncoated product.

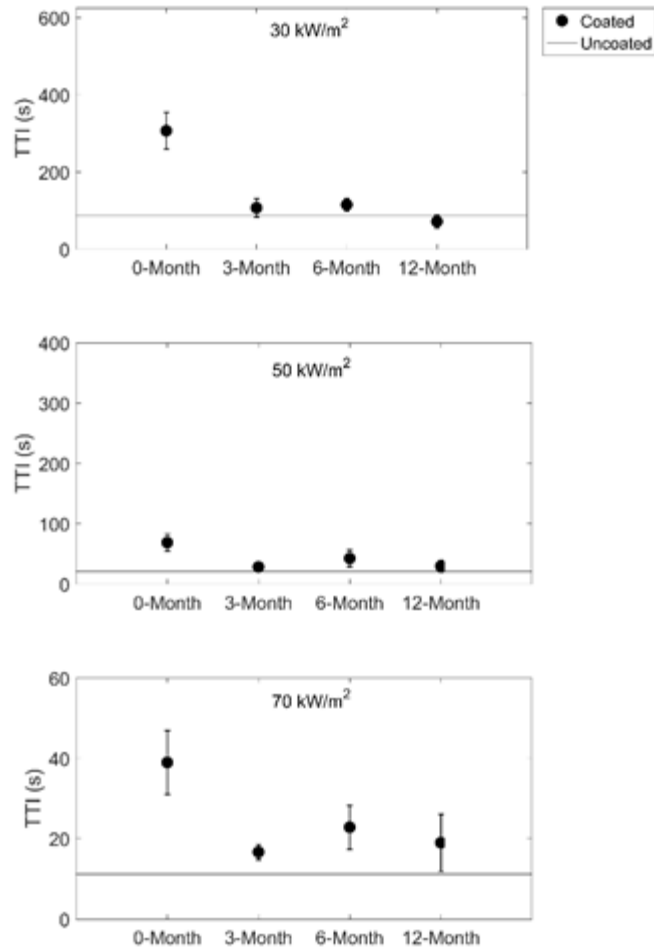


Figure 23. TTI for Coating A at each weathering period and heat exposure level. The error bars on each plotted point show ± 1 standard deviation. The horizontal line represents the average value for the uncoated specimen, +1 standard deviation.

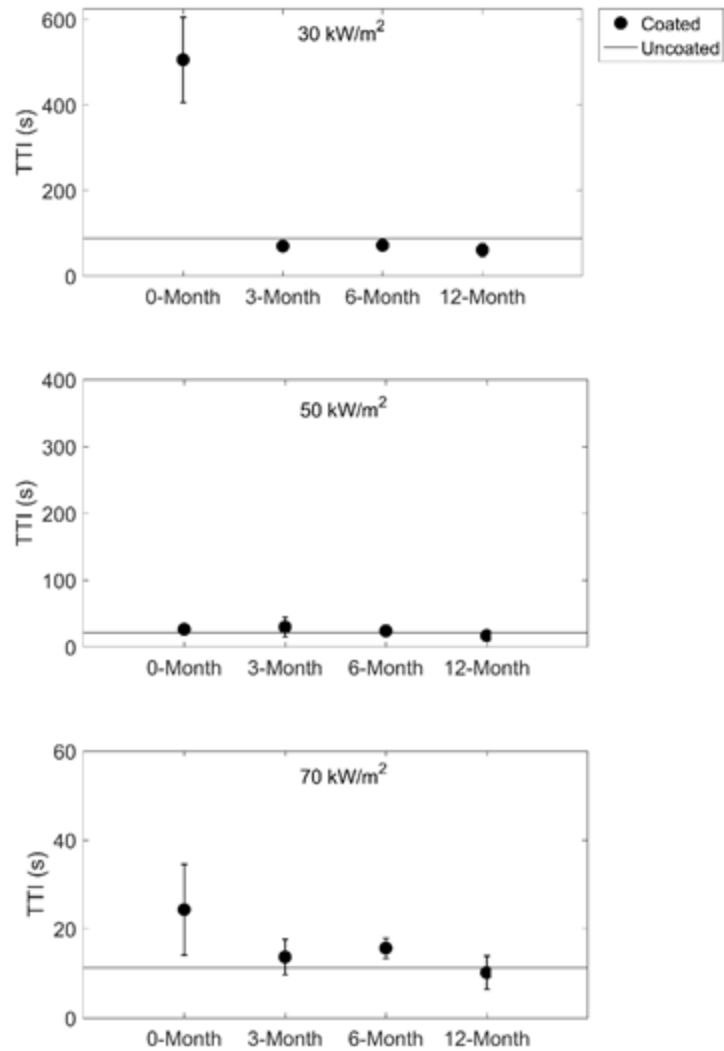


Figure 24. TTI for Coating B at each weathering period and heat exposure level. The error bars on each plotted point show ± 1 standard deviation. The horizontal line represents the average value for the uncoated specimen, +1 standard deviation.

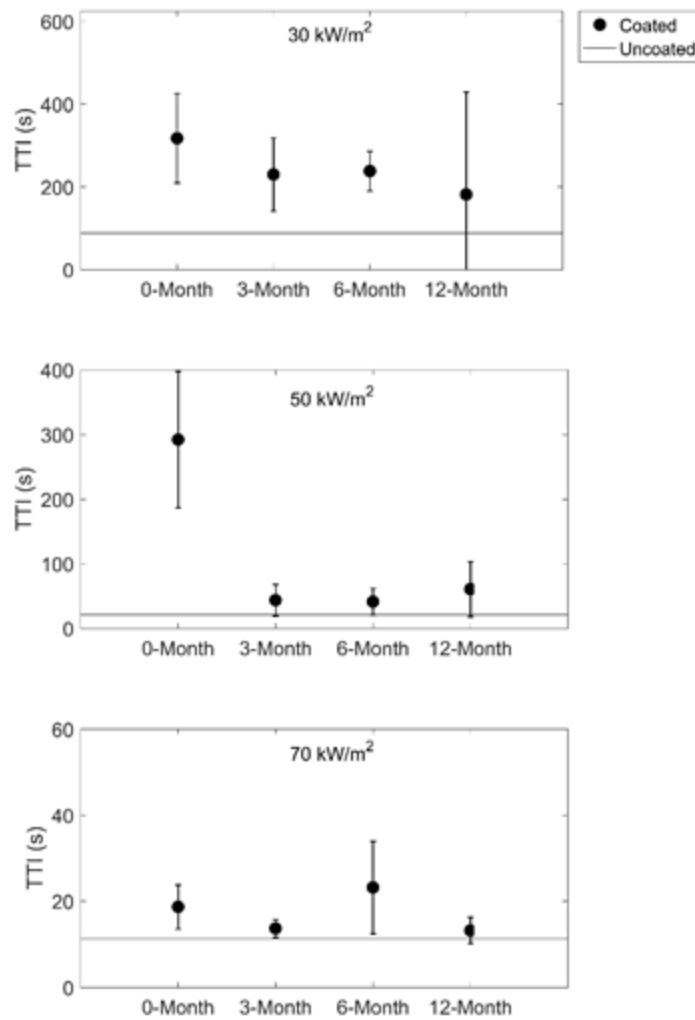


Figure 25. TTI for Coating C at each weathering period and heat exposure level. The error bars on each plotted point show ± 1 standard deviation. The horizontal line represents the average value for the uncoated specimen, +1 standard deviation.

Analysis of Paint Film Thickness

The paint film thicknesses for Coatings A, B, and C were measured for the 0-, 3-, and 6-month weathering periods, both northern and southern exposures. For each coating, a total of three specimens were used to measure paint film thickness. For each specimen selected for analysis, two samples were created as shown in Figure 4. Since the samples were created by using a hot-melt adhesive to face-glye two smaller pieces, thickness was measured both above and below the glued interface. Both long edges of each sample were prepared, following specifications in ASTM D5235-14 (2014), and measured. This procedure resulted in 16 measurements per sample, a total of 32 paint

film thickness measurements per specimen. The average of the thickness measurements was calculated.

It should be noted that the average paint film thickness measurements were based on instances where coating thickness could be measured. Cracks began to form in aged specimens as discussed earlier in the surface evaluation section of this report. If a void or surface check were present in the coating as shown in Figure 26, no measurement of thickness was taken. Also, due to sanding of the samples during preparation, there were some instances where no coating was observed and, therefore, the average thickness was taken from fewer than 32 measurements.

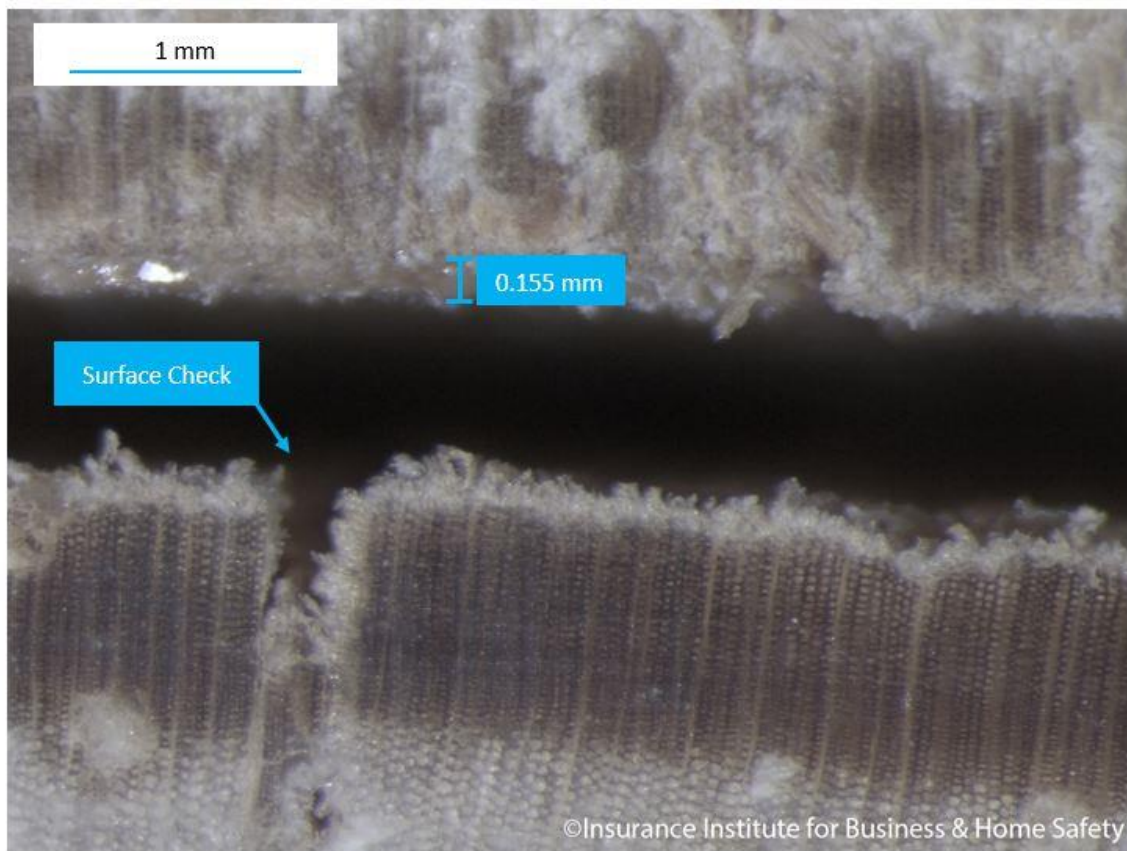


Figure 26. Example of a surface check in the plywood substrate.

As also stated previously in this report, an analysis to assess changes in the chemical makeup of the coating as a function of weathering was not performed. Thus, it is hypothesized that any cracks in the coating due to chemical changes in the coating over time would expose the unprotected substrate and likely explain a reduction in fire performance properties of the coating.

Film-Forming Coating A

The results of the measured paint film thickness analysis for Coating A are shown in Figure 27. Coating A was glossy in appearance when initially applied. While it was a clear coating, its thickness could be discerned when viewed under the microscope. On average, the coating was thickest when initially applied. When considering the variability in thickness—as indicated by the error bars shown in Figure 26—thickness did not measurably change over the course of the experiment, even when considering weathering periods and orientation. The variability in thickness can more accurately be attributed, therefore, to the fact that the coatings were applied to each plywood panel by hand.

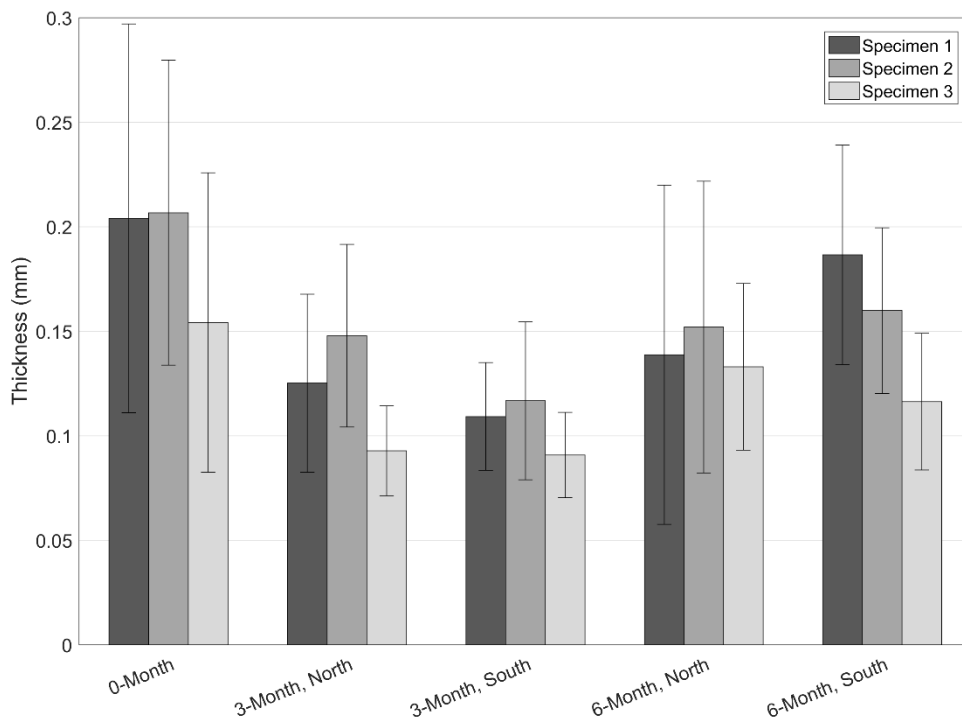


Figure 27. Measured paint film thickness analysis for Coating A. Note: 1 mm = 0.039 in.

Film-Forming Coating B

The results of the measured paint film thickness analysis for Coating B are shown in Figure 28. Specimens for this coating had several cracks that formed in the 3-month weathering period, as well as subsequent weathering periods. As with Coating A, there were instances where the average thickness was taken from less than 32 measurements. The magnitude of the thickness was similar for the 0-, 3-, and 6-month weathering periods, both north and south oriented specimens. A reduction in coating thickness as a function of weathering was not observed.

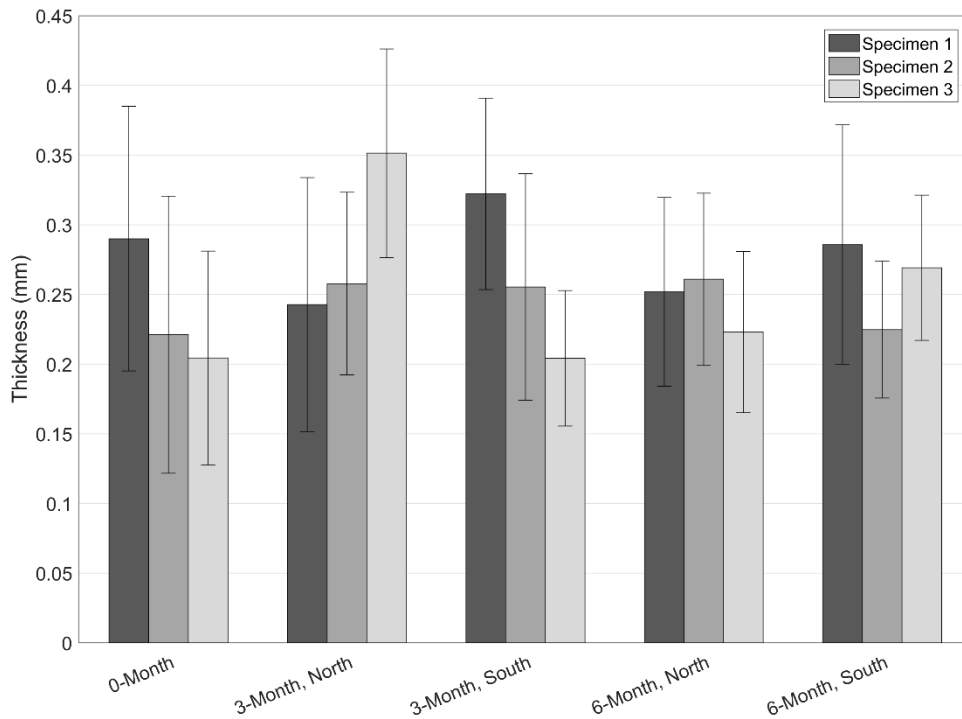


Figure 28. Measured paint film thickness analysis for Coating B. Note: 1 mm = 0.039 in.

Film-Forming Coating C

The results of the measured paint film thickness analysis for Coating C are shown in Figure 29. One sample experienced a reduction in thickness, but the overall trend as observed with the other coatings was that film thickness remained relatively constant during the 12-month weathering period. Based on qualitative observations, this coating performed the best with limited discoloration, cracking, or mold growth.

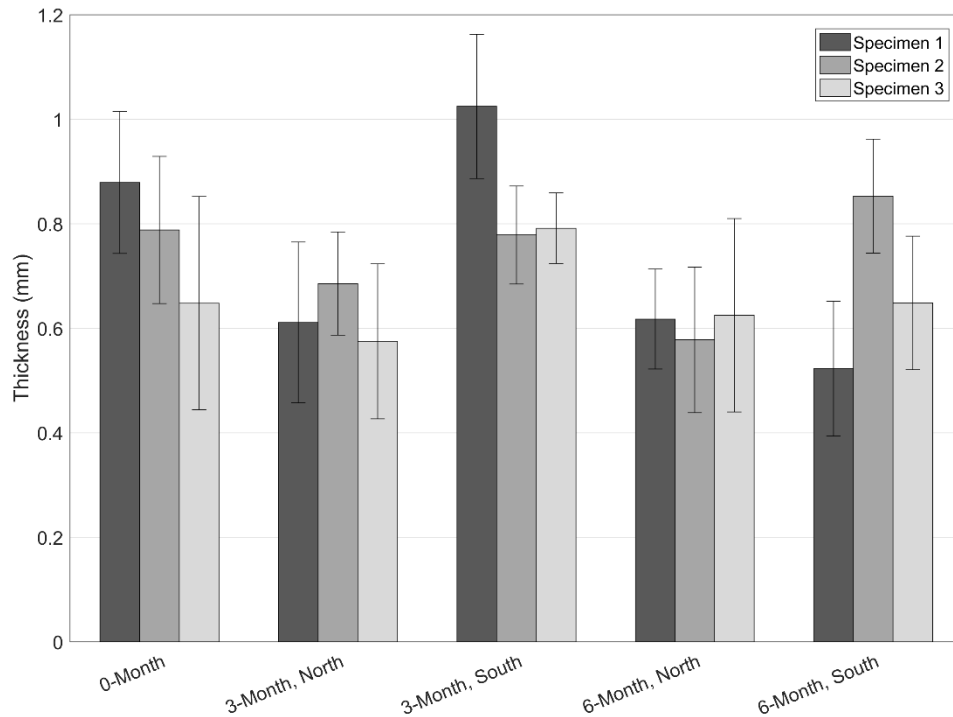


Figure 29. Measured paint film thickness analysis for Coating C. Note: 1 mm = 0.039 in.

Summary of Paint Film Thickness Analysis

The paint film thickness evaluation was conducted on samples created from specimens for the three film-forming coatings (A, B, and C). Film thickness measurements and other qualitative, visual observations were made for specimens after the 0-, 3, 6-, and 12-month weathering periods. The penetrants showed signs of discoloration and mold growth between the weathering periods for 6 and 12 months. Coatings A and B began to exhibit cracking after three months of weathering. The surfaces of these coatings were beginning to flake after 12 months, exposing the plywood substrate. Coating A also had noticeable discoloration and mold growth. In terms of visual durability, Coating C had the best product performance with limited cracking up to 12 months.

Summary and Conclusions

The performance of three film-forming coatings and two penetrant coatings were evaluated. Fire tests in a cone calorimeter were conducted on intumescent- and fire-retardant-coated specimens to assess the performance of the coating products after natural weathering. The condition of the coatings after weathering was also assessed. This included a qualitative evaluation of changes in the surfaces of all coating and an analysis of changes in paint film thickness for the film-forming coatings only.

The TTI data was analyzed using an analysis of variance (ANOVA) procedure. This analysis indicated that there was no significant difference between northern and southern exposures ($\alpha = 0.05$), therefore, these data were combined.

Literature provided by the coating manufacturers claimed that each respective product would have an effective service life of up to five years when used in an exterior environment. Results from this study indicated that none of the products retained their fire-retardant properties for an extended period when used in an exterior environment.

Results from this study indicated that none of the products retained their fire-retardant properties for extended periods when used in an exterior environment.

The non-weathered penetrant coating products (D and E) did not enhance fire retardant performance over uncoated wood. None of the film-forming coating products (A, B, and C) enhanced fire performance over the uncoated samples after even the 3-month weathering period. At least with current formulations, none of the coating products included in this experiment can be relied on to provide enhanced protection from radiant heat exposures over an uncoated product.

References

- ASTM D5235. (2014). Standard Test Method for Microscopic Measurement of Dry Film Thickness of Coatings on Wood Products, ASTM International, West Conshohocken, PA. doi: 10.1520/D5235-14.
- ASTM E1354. (2015). Standard Test Method for Heat and Visible Smoke Release Rates for Materials and Products Using an Oxygen Consumption Calorimeter, ASTM International, West Conshohocken, PA. doi: 10.1520/E1354-15A.
- Bahrani, Babak. (2015). Effects of Weathering on Performance of Intumescent Coatings for Structure Fire Protection in the Wildland-Urban Interface. A thesis submitted to the faculty of The University of North Carolina at Charlotte in partial fulfillment of the requirements for the degree of Master in Fire Protection and Administration. Charlotte, NC. 128 pp.
- California Building Code, 2009. Chapter 7A [SFM] Materials and Construction Methods for Exterior Wildfire Exposure. Retrieved from http://www.fire.ca.gov/fire_prevention/downloads/ICC_2009_Ch7A_2007_rev_1Jan09_Supplement.pdf. Last accessed March 15, 2017.
- Gorte, R. (2013). The Rising Cost of Wildfire Protection. Headwaters Economics Research Paper. Headwaters Economics. Bozeman, MT. 15 pp.
- Maranghides, A., McNamara, D., Vihnanek, R., Restaino, J., and Leland, C. (2015). A Case Study of a Community Affected by the Waldo Fire – Event Timeline and Defensive Actions. NIST Technical Note 1910. National Institute of Standards and Technology.
- Schartel, B., Hull, T.R. (2007). Development of fire-retarded materials - interpretation of cone calorimeter data. *Fire and Materials*. pp. 327-354.
- Short, J.R. (2015). The West is on fire – and the US taxpayer is subsidizing it. *The Conversation*. Retrieved from <https://theconversation.com/the-west-is-on-fire-and-the-us-taxpayer-is-subsidizing-it-47900>. Last accessed March 15, 2017.
- Wang, Y., Göransson, U., Holmstedt, G., and Omrane, A. (2005). A Model for Prediction of Temperature in Steel Structure Protected by Intumescent Coating, Based on Tests in the Cone Calorimeter. *Fire Safety Science – Proceedings of the Eighth International Symposium*. pp. 235-246.

White, R.H., Dietsberger, M.A. (2010). Fire Safety of Wood Construction. In: *Wood Handbook, Wood as an Engineering Material*. General Technical Report FPL-GTR-190. U.S. Department of Agriculture, Forest Service, Forest Products Laboratory. Madison, WI. 508 pp.

Appendix A

Table A1. Cone calorimeter result averages for Coating A.

Weathering Period	Orientation	Heat Flux Level (kW/m ²)	TTI (s)	T _{intu} (s)	PHRR (kW/m ²)
0-Month	N/A	30	385	23	164
		50	69	17	206
		70	39	9	252
3-Month	North	30	109	67	214
		50	29	26	281
		70	17	13	312
	South	30	105	60	215
		50	28	23	266
		70	16	12	269
6-Month	North	30	119	60	189
		50	39	24	276
		70	27	14	328
	South	30	111	65	177
		50	46	31	231
		70	19	15	312
12-Month	North	30	69	-	170
		50	29	-	289
		70	20	-	340
	South	30	74	-	200
		50	31	-	223
		70	18	-	354

Table A2. Cone calorimeter result averages for Coating B.

Weathering Period	Orientation	Heat Flux Level (kW/m²)	TTI (s)	T_{intu} (s)	PHRR (kW/m²)
0-Month	N/A	30	506	64	179
		50	26	22	190
		70	24	14	228
3-Month	North	30	66	-	247
		50	42	31	331
		70	11	-	293
	South	30	73	-	187
		50	18	-	290
		70	16	-	338
6-Month	North	30	82	-	153
		50	18	-	242
		70	16	-	351
	South	30	61	-	205
		50	31	-	325
		70	16	-	345
12-Month	North	30	66	-	237
		50	17	-	324
		70	13	-	228
	South	30	56	-	208
		50	17	-	347
		70	7	-	404

Table A3. Cone calorimeter result averages for Coating C.

Weathering Period	Orientation	Heat Flux Level (kW/m²)	TTI (s)	T_{intu} (s)	PHRR (kW/m²)
0-Month	N/A	30	317	46	130
		50	292	42	208
		70	19	11	192
3-Month	North	30	250	50	149
		50	48	22	234
		70	13	11	262
	South	30	199	53	39
		50	39	19	248
		70	14	11	199
6-Month	North	30	255	42	179
		50	45	22	146
		70	28	12	262
	South	30	211	49	32
		50	30	27	25
		70	19	13	286
12-Month	North	30	209	-	13
		50	74	-	182
		70	14	-	232
	South	30	153	-	77
		50	47	-	192
		70	12	-	279